Impact of strongback on structure with varying damper and stiffness irregularity arrangements

Sima Abolghasemi, Nicholas Wierschem*, and Mark D. Denavit

Department of Civil and Environmental Engineering, University of Tennessee, Knoxville, TN, USA

*Corresponding Author, nwiersch@utk.edu, 851 Neyland Drive Knoxville TN 37996-2313

Abstract

Structures susceptible to soft story mechanisms are particularly vulnerable to earthquakes because damage concentrated at a single story can lead to premature failure of the structure. The strongback, a stiff vertical spine pinned at the structure's base and running its height, has been proposed as a way to impose a more uniform pattern of floor displacements and prevent soft story mechanisms. However, changes in the impact of strongbacks on the performance of structures remain unclear when considering vertical stiffness irregularities at different positions along the height of a structure and different arrangements of energy dissipation devices in a structure. This study aims to address these gaps through an extensive parametric experimental investigation varying the location of vertical stiffness irregularities and the arrangement of dampers in a small-scale four-story elastic structure with and without a strongback. For this study, each configuration of the structure is loaded with shake table-produced seismic ground motion. The results of this study show that, regardless of which story a stiffness irregularity is located, the strongback significantly reduces the maximum story drift in the structure. Furthermore, with the strongback, the maximum story and roof drift are insensitive to damper position and distribution, whereas, without it, the damper position significantly impacts the structural performance. The strongback's ability to protect against soft story vertical irregularities, regardless of their locations, and the insensitivity of structural performance to damper arrangement when utilizing a strongback, presents promising new options for structural design, architectural design, and remediation efforts.

Keywords: Strongback, soft story mechanism, damper arrangement, stiffness irregularity, experimental

1. Introduction

Structures susceptible to soft story mechanisms are particularly vulnerable to earthquakes as these mechanisms result in localized damage concentration and the non-ductile premature failure of the structure. Connecting a vertical elastic spine, also known as a strongback, to a primary structural system is one proposed method to prevent the formation of soft story mechanisms. Elastic spines have also been proposed to help address vertical structural irregularities in design.

The strongback is a stiff and strong element or group of elements that is pinned at the base of a structure and runs the height of the structure. As a result, the strongback experiences rigid body motion when the structure has uniform drift, but provides significant resistance to any other pattern of drifts, such as those that would be present with a soft story mechanism. By preventing premature failure due to a soft story mechanism, the strongback is intended to help structures have an overall more ductile response [1], [2].

The fundamental concept behind the strongback, imposing a displacement pattern to reduce or prevent the concentration of damage, has been studied under different names as well, including the hinged wall [3], rocking steel shear wall [4], [5], spine frame [6]–[8], stiff rocking core [9], and vertical rigid truss [2], [10]. Furthermore, some basic structural elements, including continuous columns [11], have been identified as possessing similar capabilities as the strongback, imposing a displacement pattern, if designed with sufficient stiffness and strength.

The efficient design of strongbacks and other types of elastic spines is an area of current research. Design by nonlinear response history analysis is an option but is difficult to implement in practice. Simplified modal pushover analysis [12] and generalized modified modal superposition [13] are among the simpler methods that have been proposed specifically for the design of strongback systems. Both methods consider the higher mode effects and partial yield mechanisms that can complicate strongback design. With the formation of a global plastic mechanism being a primary goal of strongback systems, the theory of plastic mechanism control [14] may also be well-suited for their design. However, none of these simpler methods have been included in design standards yet.

Many numerical studies have investigated the performance of systems that behave like strongbacks [1], [10], [15], [16], but experimental studies on these systems are limited. Simpson and Mahin [2] studied the weak-story behavior of a nearly full-scale two-story structure with a strongback that effectively delayed or prevented soft-story formation even after the rupture of the structure's buckling-restrained braces. Hu et al. [7] studied a self-centering companion spine composed of two rigid spines and friction dampers to enhance structural response and mitigate damage during seismic events using an experimental structural model based on a length scale of 0.35. A collaborative study conducted by a U.S.-Japan team [17] focused on the full-scale testing of a frame-spine system with force-limiting connections added to a moment-resistant frame. Due to the large scales considered and other experimental complexities, the majority of the experimental works related to strongbacks have featured a small number of tests or a single test; thus, wider-ranging experimental parametric studies on structures with strongbacks have not been performed. The stiffness of the strongback and the stiffness of the primary structure (i.e., the structure into which the strongback is incorporated) are both important and impact the behavior of the combined system. Chen et al. [15] numerically investigated the impact of strongback stiffness and strength on the behavior of a three-story special concentrically braced frame with an attached strongback. Lin et al. [18] conducted a numerical study on several stiffness configurations for the strongback, considering both the overall stiffness of the strongback and the distribution of stiffness in the strongback. This work also investigated the effectiveness of the strongback for different primary structure types: a three-story shear deformation-dominated structure and a nine-story flexure deformation-dominated structure. Other work explicitly considered the impact of a strongback on a structure with a story with reduced stiffness [2], but this work did not vary the position of the soft story vertical irregularity in the structure. Consequently, investigations focusing on the effectiveness of the strongback given changes to the primary structure's stiffness are limited.

There have been many investigations on improving structural behavior and mitigating soft-story mechanisms through the use of energy dissipation devices [19], [20] and buckling restrained braces [21], [22]. The effects of including different types of energy dissipation devices in structures with strongbacks have also been considered. Qu et al. [23] investigated the effectiveness of shear-type steel dampers that were distributed throughout the height of an eleven-story steel-reinforced concrete frame with pin-supported walls. Wang et al. [24] also investigated a pin-supported wall frame structure and considered hysteretic and viscoelastic dampers in this structure. Hu et al. [7] proposed the use of friction spring dampers with recentering properties that were distributed along the height of a steel structure that featured a pair of rigid spines. Palermo et al. [10] numerically investigated a structure with a strongback and several configurations of viscous dampers in the structure, including dampers at each story, at some select stories, and concentrated vertically at the base of the strongback. This work concluded that the strongback's presence allowed for the increase in seismic performance effectiveness of these different configurations of viscous dampers due to a more uniform potential for energy dissipation by dampers located throughout the height of the structure. While some studies have investigated the impact of damper configurations in a strongback system, the effect of concentrating all of the structure's dampers in one story and the effect of the location of that damped story, have not been widely considered or experimentally investigated. This is an important gap in knowledge as the ability to concentrate dampers at a single story can add desirable design flexibility.

The objective of this work is to determine the effect of the position of stiffness irregularities in a primary structure and the arrangement of dampers in the structure on the dynamic performance and properties of a structure with a strongback. This experimental investigation was performed with a small-scale four-story model structure with and without an attached strongback subjected to shake table-produced ground motion. This investigation is composed of an experimental parametric analysis that considers the location of stiffness irregularities, produced by reducing the column thickness in specific stories, and considering the arrangement of dampers in different stories of the structure. The scale and limited complexity of the model enabled this experimental parametric analysis to consider more system configurations and ground motions than other experimental studies on strongback systems. The impacts of the stiffness irregularities and damper arrangement are evaluated considering the resulting maximum story and roof drift of the structure as well as changes in the structure's first natural frequency and first mode damping coefficient. Data from these tests were used to develop an understanding of how the dynamic behavior and response of the structure changes due to the stiffness irregularities and damper arrangement with and without the strongback.

This paper is organized as follows. Section 2 describes the primary structure and strongback used in this experimental study. Section 3 presents the system configurations considered to investigate the effects of stiffness irregularities and the arrangement of dampers in the structure. Furthermore, this section describes the ground motions considered and the instrumentation used to measure the response of the structure. The results of the experimental parametric investigation are presented and discussed in Section 4, where they are divided into a study investigating the effects of stiffness irregularities and a study investigating the impact of damper arrangements. In Section 5, the results of the studies are summarized, and conclusions are presented.

2. Physical Model

The physical model used in this work was a four-story structure (referred to as the primary structure) with a strongback attached to it. An isometric view of the physical model is shown in Figure 1. Figure 2 shows an elevation view of the physical model and is annotated with key dimensions. Details on the structure dimensions not shown in Figure 1 and Figure 2 can be found in the design drawings for this structure [25]. Tests were performed on this physical model with and without the strongback attached to the primary structure. In order to avoid damage and enable a large parametric study with this model, this structure was designed to remain elastic during testing.

Each of the four floors and the base of the primary structure was a 457.2 mm x 457.2 mm x 12.7 mm 6061-T6511 aluminum plate. Grade 1095 spring steel columns were located in the corners of the structure and bolted to the sides of the plate, forming a moment-resisting connection. The columns were 50.8 mm wide and had a thickness of either 1.575 mm (original thickness) or 1.067 mm (reduced thickness). The columns were oriented in the same direction such that the overall structure was flexible in one lateral direction and stiff in the orthogonal lateral direction, and the connections were such that the bending span of the columns was the clear story height. The center-to-center height of each story was 244.5 mm and the clear story height was 231.8 mm. The flexural rigidity, EI, of the spring steel columns, was determined through a three-point bending test as EI = 3.205 N-m^2 and 1.049 N-m^2 for the original and reduced thickness columns, respectively.

The strongback was constructed from two 76.2 mm wide and 12.7 mm thick aluminum plates. The plates were joined together by several connector pieces. The strongback was pinned at the base using a partially threaded bolt. The centerline of the strongback pin was at the same elevation as the centerline of the base plate. The strongback was attached to the primary structure at each floor with aluminum link arms with cross-sectional dimensions of 38.1 mm width and 12.7 mm thickness that were pinned at the strongback (left arm pin) and brackets (right arm pin). The brackets were rigidly connected to the floor plates. The centerline of the right arm pins was at the same elevation as the centerline of the floor plates. Due to a design error, the center-to-center spacing of the left arm pins was 241.3 mm, less than the story height of the primary structure, resulting in the arms being slightly tilted when the structure is in its undeformed position. The strongback was oriented such that it rotated about its base pin with motion in the flexible direction of the primary structure.

The mass of each floor, including associated hardware (e.g., the bracket, but not the link arm), was 8.083 kg. The mass of each of the original thickness columns was 0.154 kg. The mass of each of the reduced thickness columns was 0.113 kg. The mass of each link arm was 0.576 kg. The mass of the strongback, including associated hardware, was 10.156 kg. The center of gravity of the strongback was 568.3 mm above the center of the strongback pin. In cases when the strongback is not present, the strongback, link arms, and associated hardware were removed, but the brackets connected to the floor plates remained.

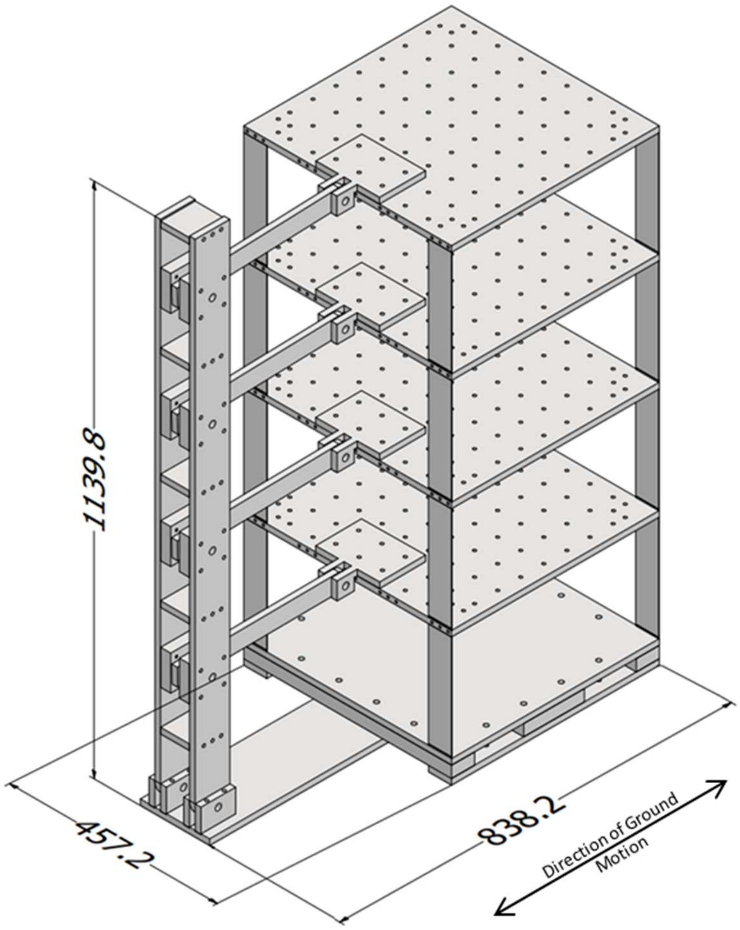

Figure 1: Isometric view of the physical model of the primary structure with the strongback– units are mm

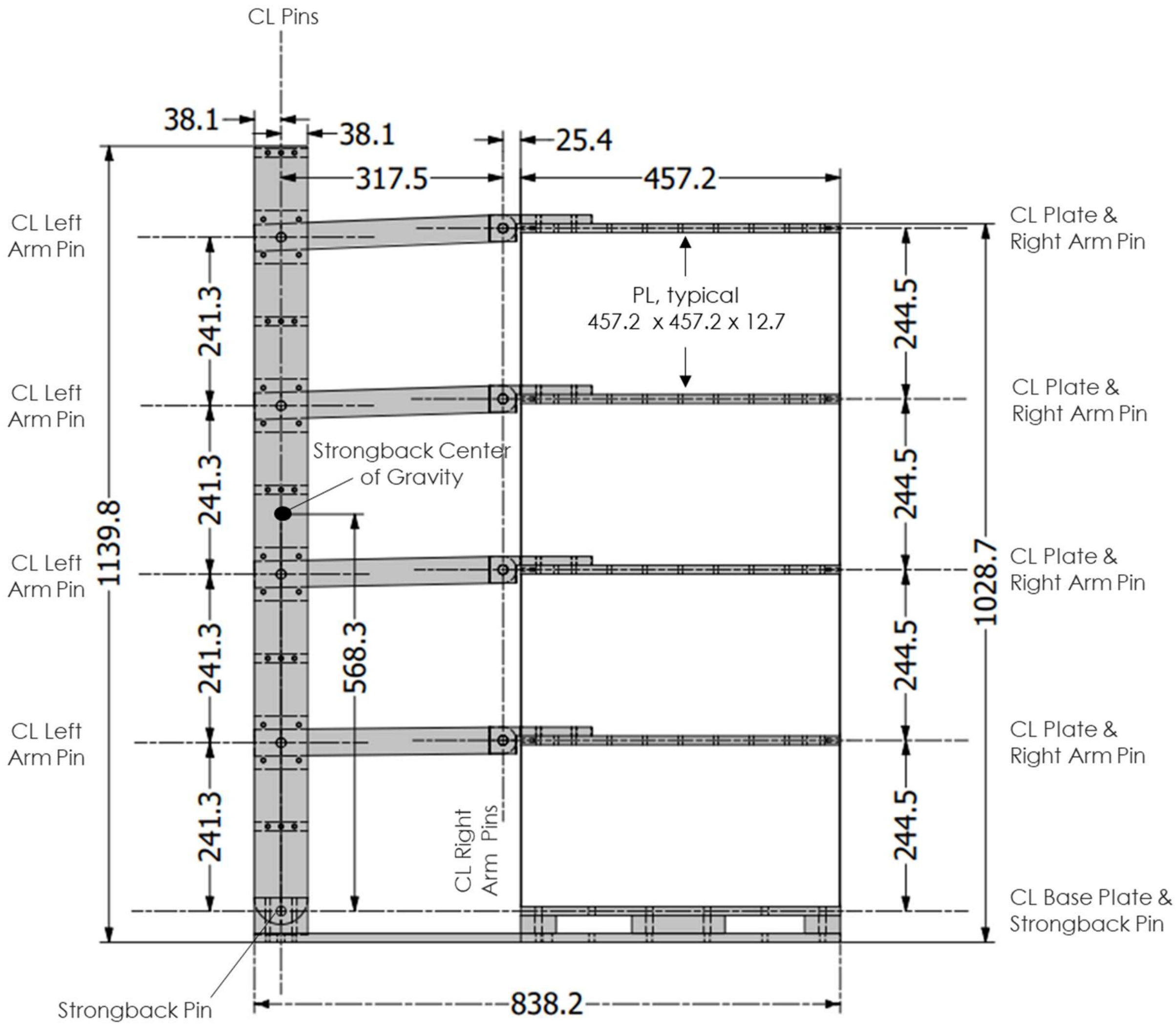

Figure 2: Dimensioned elevation view of the primary structure with the strongback – units are mm, CL = centerline

The dampers used in this study were shock absorbers that were repurposed from an intended use in hobby radio-controlled cars. These devices provide damping through the dynamic motion of a plunger through an oil-filled chamber. The dampers were filled with 30-weight oil, which was determined to be an appropriate viscosity based on a preliminary investigation. The properties of each of the four dampers used in this study were characterized in a separate single-degree-of-freedom test structure subjected to shaped random ground motion. Each damper was pin connected to two sets of aluminum mounts fixed to the test structure's top and bottom plates. From these tests, the average effective viscous damping provided by a single damper was identified to be 77±23 Ns/m. The variability in the estimated effective viscous damping existed for the different dampers as well as the same damper in repeated trials.

A pair of aluminum brackets were used to connect each damper between floors of the primary structure. The mass of a single damper with brackets and associated hardware was 0.733 kg. When considering a distributed arrangement of the dampers, a damper was placed in each story of the primary structure at the centerline of the floor and orientated in the flexible direction of the structure. When considering concentrated arrangements of the dampers, all four dampers were placed in a single story, arranged symmetrically along the centerline of the floor, and orientated in the flexible direction of the structure. Figure 3 shows photos of the dampers connected in a story of the structure in the concentrated and distributed configurations.

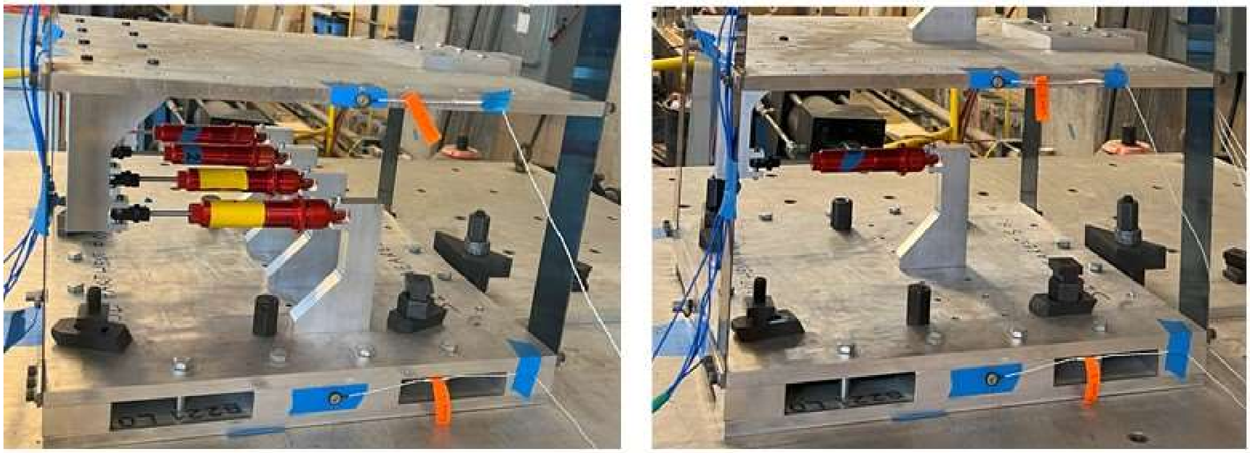

Figure 3: Dampers connected in a story of the structure. Left- Concentrated arrangement in the first story, Right- Distributed arrangement showing first story only.

3. Description of Experimental Tests

This section describes the structure configurations, ground motions, and data collected during the experimental tests.

3.1. Structure configurations

Table 1 shows the system configurations utilized for the experimental testing. To investigate the impact of stiffness irregularities on the dynamic performance of the model structure, tests were performed for configurations where reduced thickness columns were installed in lieu of the original thickness columns in a single story. There were eight such configurations, four (one for each story) times two (with and without strongback). Additionally, two configurations (with and without strongback) with all original thickness columns were tested as a control. No dampers were used in any of the tests investigating stiffness irregularities.

To investigate the impact of damper arrangement, tests were performed for configurations where all four dampers were installed in a single story. There were eight such configurations, four (one for each story) times two (with and without strongback). Additionally, two configurations (with and without strongback) with the dampers distributed one per story were tested as a control. Original thickness columns were used in all stories for all tests investigating damper arrangement.

Table 1: System configurations for stiffness irregularity and damper arrangement tests

Test Type	Strongback Config.	Config. Name	Column thickness at Each Story				Number of Damper at Each Story			
			1st	2nd	3rd	4th	1st	2nd	3rd	4th
Stiffness Irregularity (SI)	No Strongback	SI1	R	O	O	O	---	---	---	---
		SI2	O	R	O	O	---	---	---	---
		SI3	O	O	R	O	---	---	---	---
		SI4	O	O	O	R	---	---	---	---
		NSI	O	O	O	O	---	---	---	---
	Strongback (SB)	SI1-SB	R	O	O	O	---	---	---	---
		SI2-SB	O	R	O	O	---	---	---	---
		SI3-SB	O	O	R	O	---	---	---	---
		SI4-SB	O	O	O	R	---	---	---	---
		NSI-SB	O	O	O	O	---	---	---	---
Damper Arrangement	No Strongback	DC1	O	O	O	O	4	---	---	---
		DC2	O	O	O	O	---	4	---	---
		DC3	O	O	O	O	---	---	4	---
		DC4	O	O	O	O	---	---	---	4
		DDA	O	O	O	O	1	1	1	1
	Strongback (SB)	DC1-SB	O	O	O	O	4	---	---	---
		DC2-SB	O	O	O	O	---	4	---	---
		DC3-SB	O	O	O	O	---	---	4	---
		DC4-SB	O	O	O	O	---	---	---	4
		DDA-SB	O	O	O	O	1	1	1	1
O: Original column thickness R: Reduced column thickness										

As seen in Table 1, SI1, SI2, SI3, and SI4 refer to configurations without the strongback and with the stiffness irregularity in the first, second, third, and fourth stories, respectively. NSI refers to the configuration with no stiffness irregularity in the primary structure and without the strongback. DC1, DC2, DC3, and DC4 indicate configurations without the strongback and dampers concentrated in the first, second, third, and fourth stories, respectively. DDA refers to the distributed damper configuration where all stories have one damper and without the strongback. The same configurations, but with the strongback, are denoted with “-SB” appended to the configuration name.

3.2. Ground motions

A 6 degree-of-freedom shake table at the University of Tennessee was used to provide ground motions for this testing. This table is 1.2 m x 1.2 m and was designed and built by Shore Western Manufacturing.

To avoid biasing the results of this study towards a single earthquake record, six seismic ground motions were used to assess the differences in the seismic response of the structural configurations shown in Table 1, specifically story and roof drift. The six records chosen were recorded from historic events and were obtained from the Pacific Earthquake Engineering Research Center (PEER) ground motion database [26], and some have been widely used for shake table testing [27], [17], [28]–[33]. In all cases, only component A, as denoted in the PEER database, of the recorded ground motions was used. These ground motions were applied as unidirectional horizontal motions by the shake table in the flexible direction of the structure. The records were scaled down separately to an amplitude that resulted in significant motion of the physical model without damaging it. While the shake table is unable to perfectly replicate each of the ground motions, an iterative process was used before testing the structure to produce shake table commands that largely reproduce the desired ground motions. The properties of the six recorded historic seismic ground motions are provided in Table 2.

Table 2: Identifying information and properties of ground motions used for shake table tests

No.	Earthquake name	Station	Year	Mag.	Unscaled PGA max (g)	Scaled % used for the test
1	Northridge	Beverly Hills-Mulhol	1994	6.7	0.52	15
2	Kobe, Japan	Shin-Osaka	1995	6.9	0.24	20
3	Imperial Valley	El Centro Array #11	1979	6.5	0.38	30
4	Manjil, Iran	Abbar	1990	7.4	0.51	30
5	Chi-Chi, Taiwan	CHY101	1999	7.6	0.44	20
6	Landers	Coolwater	1992	7.3	0.42	20

In addition to the recorded seismic ground motions, a shaped white noise loading was employed to examine the dynamic properties of the model structure, especially its first natural frequency and first mode damping ratio. This type of load was chosen for evaluating the structure's dynamic properties as the longer duration and broadband nature of this loading allowed for estimating the system's frequency response functions with more clarity and definition. The white noise loading was generated from a 300-second random acceleration that was subjected to a lowpass filter with a cutoff frequency of 200 Hz. This load was also applied as ground motion by the shake table in the flexible direction of the structure. The white noise was scaled such that the maximum response of the structure when subjected to the white noise was comparable to that for the recorded ground motions.

Each of the seven ground motion records (six seismic records and one shaped white noise) was applied to each of the 20 structure configurations (Table 1). As a result, 140 shake table tests were performed for this study.

3.3. Instrumentation and data acquisition

PCB model 352C33SN accelerometers connected to a data acquisition system with a sampling rate of 10,240 Hz were used to capture the acceleration of the ground (shake table) and the acceleration of each floor of the structure. The accelerometers were mounted to the middle of the side of each floor plate and the base plate. These accelerometers measured the acceleration in the structure's flexible direction, which was the primary direction of motion. Additionally, two accelerometers were mounted on top of the strongback and orientated to measure along both horizontal directions. These acceleration measurements were primarily used to estimate the structures' natural frequency and damping.

The displacement response of each floor plate, the base plate, and the strongback were captured using an NDI Optotrak, an optical measurement system that tracks emitted infrared light from markers placed on these components. This system used a sampling rate of 50 Hz. The absolute position of each marker was measured in three dimensions with a separate data acquisition system and synchronized with the acceleration measurements in post-processing. The motion of the structure in its flexible direction was extracted from the three-dimensional marker position data. These displacement measurements were used to calculate the resulting story and roof drifts.

The arrangement of the accelerometers and infrared markers on the structure is shown in Figure 4.

The system response to the white noise was used to estimate the structure's first-mode natural frequency and damping ratio for each system configuration. Numerical frequency response functions were estimated between the roof absolute acceleration and the base absolute acceleration using the tfestimate function in MATLAB [34]. Curve fitting was then used to match a single degree-of-freedom analytical dynamic model to the numerical frequency response functions produced from the experimental data using the system identification toolbox in MATLAB [35]. This curve fit only considered the frequency response function values within ±0.5 Hz of an initial estimate of the first mode frequency. Finalized system first mode damping and natural frequency estimates were then extracted from the natural frequency and damping ratio of the fit analytical single-degree-of-freedom model.

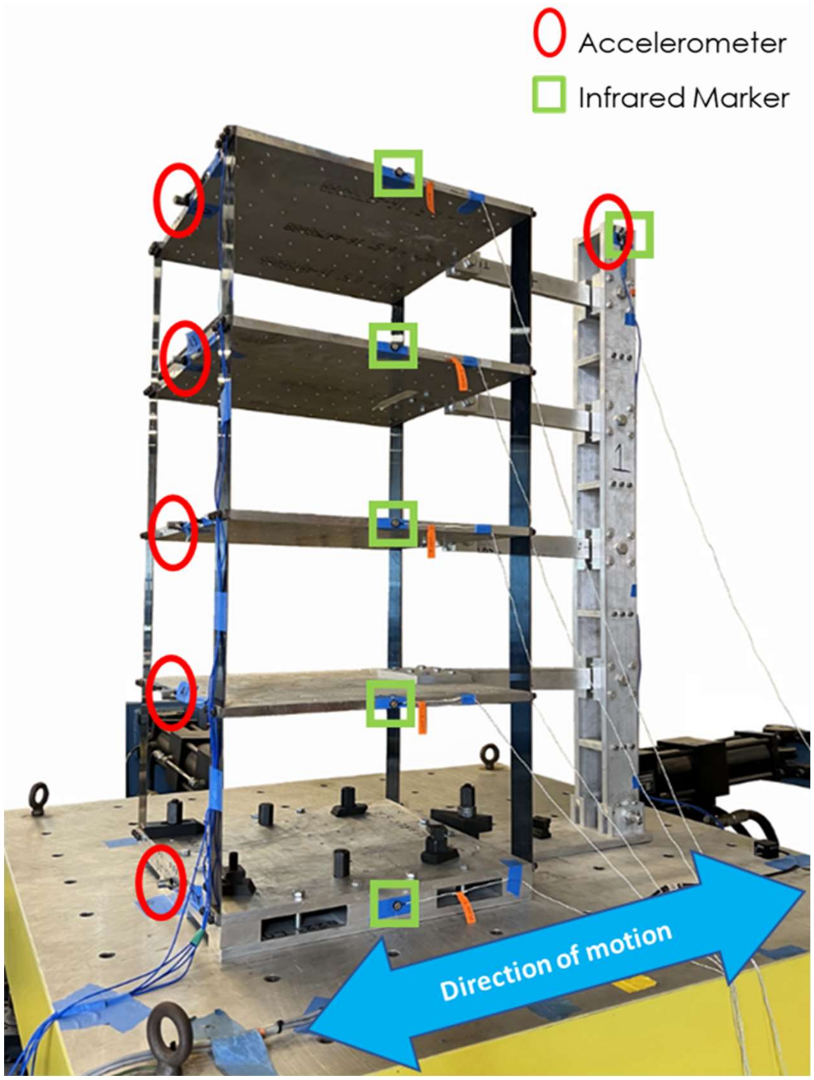

Figure 4: Primary structure with the strongback on the shake table with annotations highlighting the instrumentation

4. Results and Discussion

The experimental results and discussion thereof are divided into two parts. The first part presents and discusses results from the stiffness irregularity study and the second part presents and discusses results from the damper arrangement study.

4.1. Stiffness irregularity

The first natural frequency for each of the ten system configurations in the stiffness irregularity study (Table 1), as determined from the acceleration data from the shaped white noise tests, is shown in Figure 5. This data shows that reducing the stiffness of a story decreases the natural frequency regardless of the presence of a strongback. However, with a strongback the decrease is less pronounced. For both with and without a strongback, the decrease in natural frequency is, in general, more pronounced as reduced thickness columns are positioned in progressively lower stories of the structure.

With all original thickness columns (i.e., configurations NSI and NSI-SB), the estimated first mode frequency of the structure with the strongback is lower than without the strongback. This result is due to the additional mass provided to the system by the strongback and not the presence of a decrease in stiffness resulting from the strongback. Shifts in the first mode frequency due to stiffness irregularities are shown in Figure 5 with and without the strongback. These results show much greater consistency in the first mode frequency results for the configurations with the strongback. Specifically, the difference between the highest and lowest first natural frequency is shown to be 0.77 Hz without a strongback and 0.30 Hz when the strongback is utilized. These results suggest that the strongback can limit the impact of stiffness irregularities on the dynamic properties of the system, which may lead to more stable and predictable performance under different loading conditions.

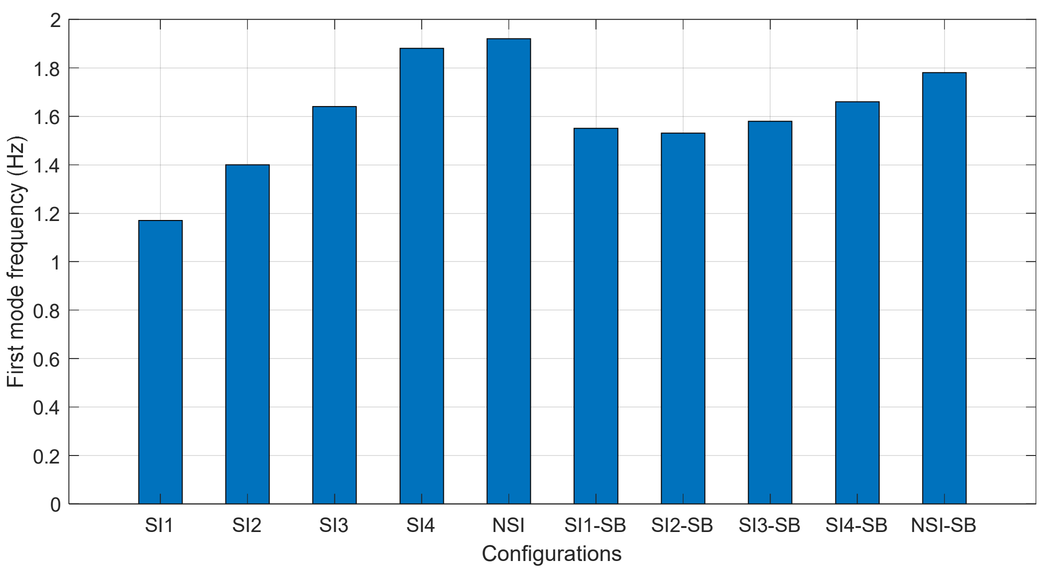

Figure 5: Estimated first mode frequency of the structure with and without the strongback given the structural configurations used for the stiffness irregularity study

Figure 6 shows the response of all the structure configurations in the stiffness irregularity study to the seven different ground motions. For each data point in Figure 6, the maximum story drift is calculated over the duration of the test and over all the stories. As seen from this figure, there is a wide range of results from the different configurations of the structure to the ground motions. As expected due to the varying nature and frequency content of the ground motions, no one configuration yields the maximum or minimum story drifts for all of the ground motions. Figure 6 does show that, in general, the presence of a strongback results in a significant reduction in the maximum story drift. While some of this reduction in maximum story drift is related to the stiffness effects of the strongback, much of this reduction can be attributed to the increased effective damping in the structure as a result of friction in the pinned joints of the strongback. While increased damping is present with the strongback in this experimental model, the strongback itself would not significantly increase damping in a realistic structure as it would not be designed to be an energy dissipating element.

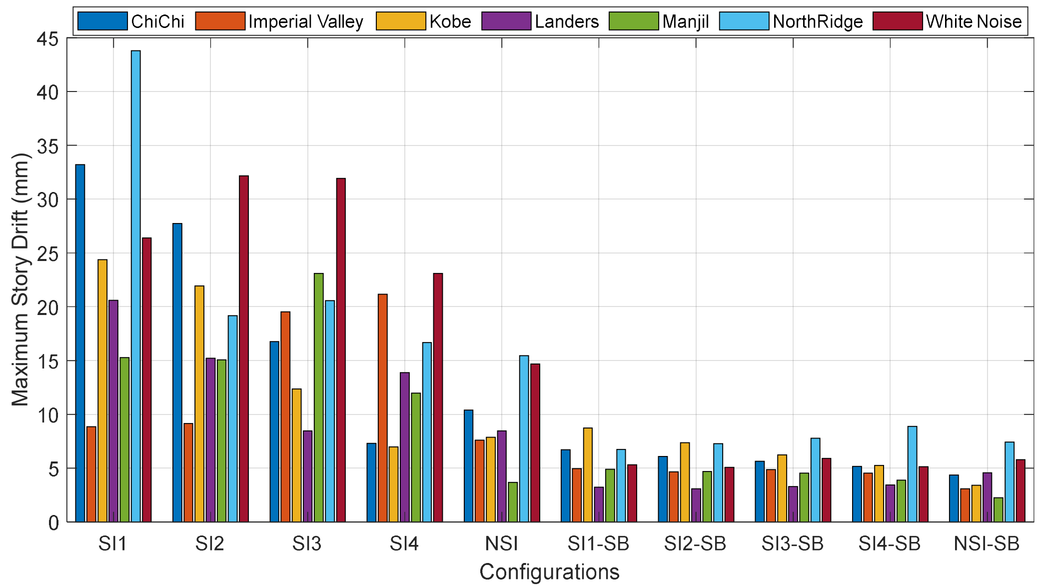

Figure 6: Maximum story drift from tests in the stiffness irregularity study.

To compensate for the damping differences in the structure with and without the strongback, the maximum story drifts for all configurations and ground motions were normalized and plotted in Figure 7. For each ground motion, the maximum story drift was normalized by dividing by the maximum story drift from configuration NSI (for configurations without the strongback) or NSI-SB (for configurations with the strongback). The use of this normalization enables identification of the impact of the stiffness irregularity on the maximum story drift, controlling for differences in mass and damping. The results in Figure 7 show that with and without the strongback, the maximum story drift, in general, increases with the presence of a stiffness irregularity and that the increase in maximum story drift grows as the stiffness irregularity is positioned lower in the structure. Furthermore, in general, the normalized maximum story drift is higher for the structure without the strongback: the peak normalized maximum drift without the strongback is 6.27 and the peak with the strongback is 2.57.

There are a number of counter-examples to the general trends discussed in the previous paragraph. This is not unexpected due to the complex interaction between the dynamics of the structure and the ground motions, which both vary in frequency content. Given this variability, rather than comparing individual test results, the average and standard deviation of the results can be considered. The average normalized maximum story drift with a stiffness irregularity is 2.25 for configurations without a strongback and 1.37 for configurations with a strongback. The standard deviation for configurations with a stiffness irregularity is 1.22 for configurations without a strongback and 0.52 for configurations with a strongback. These results show that, while the strongback is not guaranteed to have a beneficial effect; on average, it greatly reduces normalized maximum story drifts resulting from the presence of the stiffness irregularities considered.

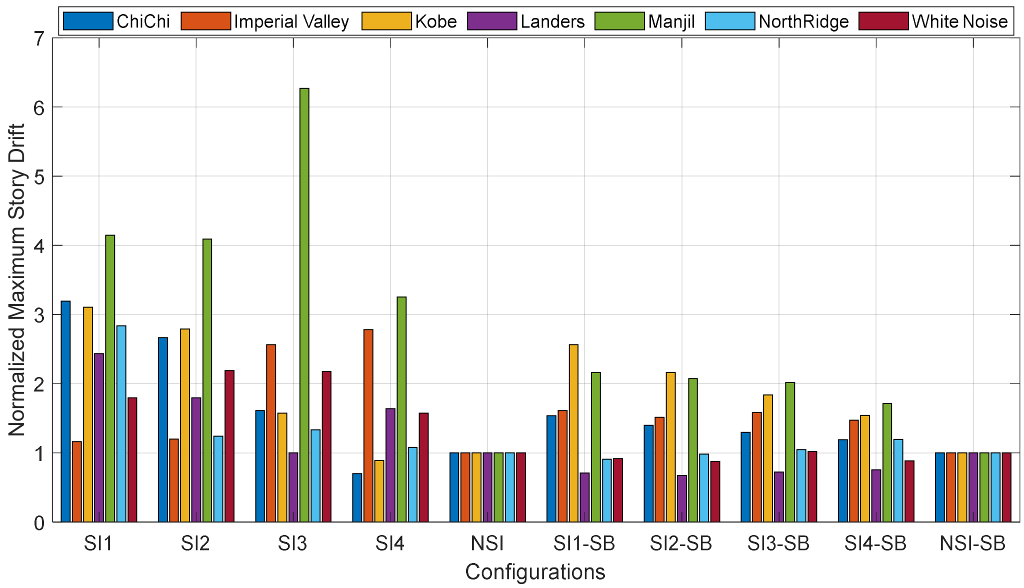

Figure 7: Normalized maximum story drift from tests in the stiffness irregularity study. Normalization of results from each record are performed with respect to the NSI configuration story drift results for systems without the strongback and with respect to the NSI-SB configuration story drift results for systems with the strongback

The maximum roof drifts for all configurations and ground motions were normalized in the same manner as for Figure 7 and are plotted in Figure 8. The peak normalized maximum roof drift without the strongback is 3.25, which is much lower than the peak normalized maximum story drift without the strongback which was 6.27, and the peak normalized maximum roof drift with the strongback is 2.57, which, when rounded, is the same as the peak maximum story drift value with the strongback. Furthermore, the average normalized maximum roof drift for configurations with a stiffness irregularity was found to be 1.38 for configurations without a strongback and 1.33 for configurations with a strongback. The standard deviation of the normalized maximum roof drift for configurations with a stiffness irregularity was found to be 0.68 for configurations without a strongback and 0.53 for configurations with a strongback. The consistency of the resulting normalized maximum story drift and maximum roof drift with the strongback indicates that the strongback imposes nearly uniform story drifts despite stiffness irregularities. In contrast, the large difference in normalized maximum story and roof drift values without the strongback is indicative of deformation concentrations.

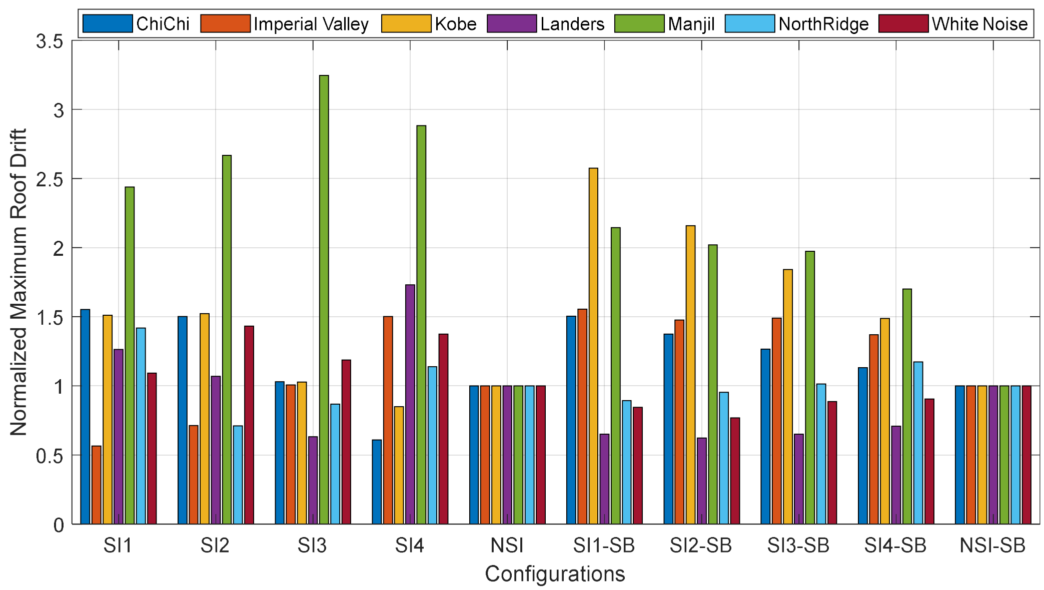

Figure 8: Normalized maximum roof drift from tests in the stiffness irregularity study. Normalization of results from each record are performed with respect to the NSI configuration roof drift results for systems without the strongback and with respect to the NSI-SB configuration roof drift results for systems with the strongback

Figure 9 shows the maximum drift for each story over the length of the excitation for all configurations in the stiffness irregularity study, with and without the strongback, and for all seismic records. This figure shows that, without the strongback, the maximum story drift is observed at the story with the stiffness irregularity. However, when a strongback is utilized, the drift is largely uniformly distributed across all stories for all seismic records. Even in the case where there is no stiffness irregularity, the presence of the strongback yields significantly more uniform story drift distribution. The results indicate that regardless of the position of the stiffness irregularity, the strongback effectively achieves uniform distribution of drift along the height of the structure.

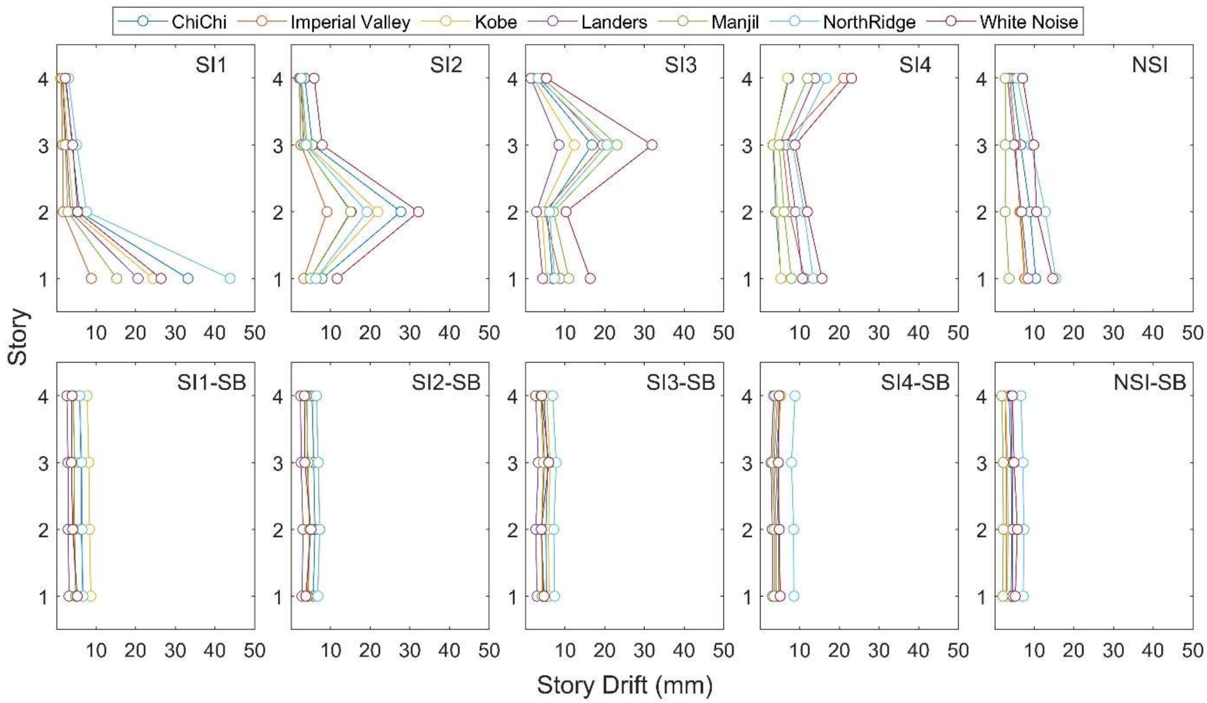

Figure 9: Story drifts with and without strongback for all configurations in the stiffness irregularity study and for all seismic records

4.2. Damper arrangement

The first natural frequency for each of the ten system configurations in the damper arrangement study (Table 1), as determined from the acceleration data from the shaped white noise tests, are shown in Figure 10. Comparing the frequencies of configurations DDA and DDA-SB in Figure 10 and configurations of NSI and NSI-SB in Figure 5, it is seen that the addition of the dampers leads to a small change in the first-mode frequency. While the addition of viscous damping does not typically change the natural frequency of structures, the dampers used in this work did not add solely pure viscous damping; rather, the dampers and their mounts have an associated mass and physical dampers have a complicated restoring force that includes stiffness effects. The results in Figure 10 shows that the first mode natural frequency increases as the location of the concentrated dampers moves down the height of the structure; however, these changes in first mode frequency are small compared to the changes observed in Figure 5 for the different locations of reduced thickness columns. Additionally, the results in Figure 10 show that the first natural frequency is lower for configurations with the strongback, which is expected due to the additional mass of the strongback.

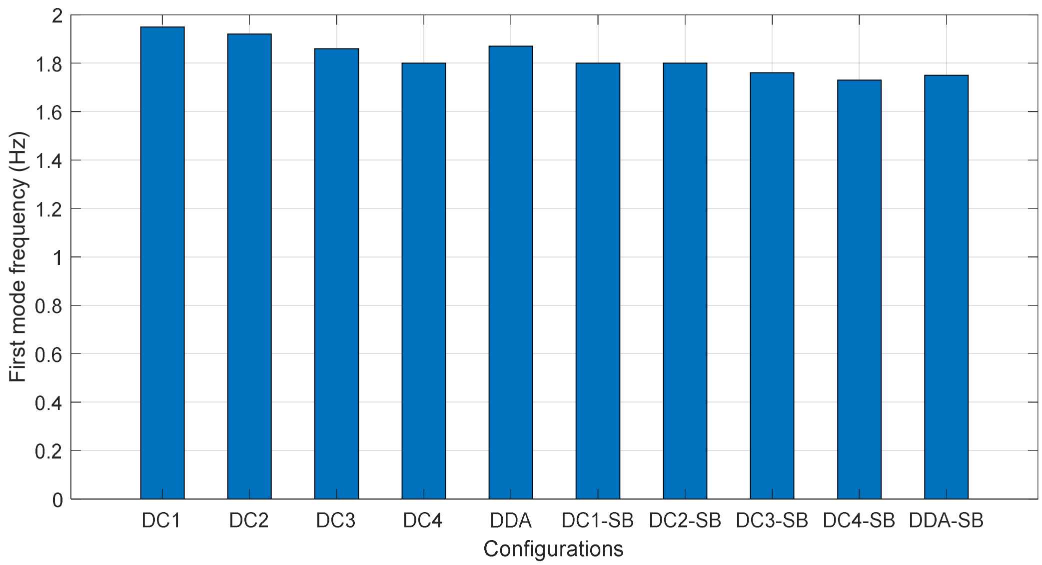

Figure 10: Estimated first mode frequency of the structure with and without the strongback given the structural configurations used for the damper arrangement study

The estimated damping associated with each configuration's first natural frequency was produced using the results with the white noise loading and are shown in Figure 11. This figure shows that with the strongback there is much higher first mode damping, which is the expected result for this model due to added frictional effects from the pins of the strongback at the base and its connections to each floor. Figure 11 also shows that the estimated damping for the configurations without the strongback change significantly with some of the concentrated damper configurations having higher estimated damping than the distributed configuration and some having lower estimated damping. In contrast, the estimated damping with the strongback is more consistent when comparing the estimated values from the concentrated and distributed damper configurations.

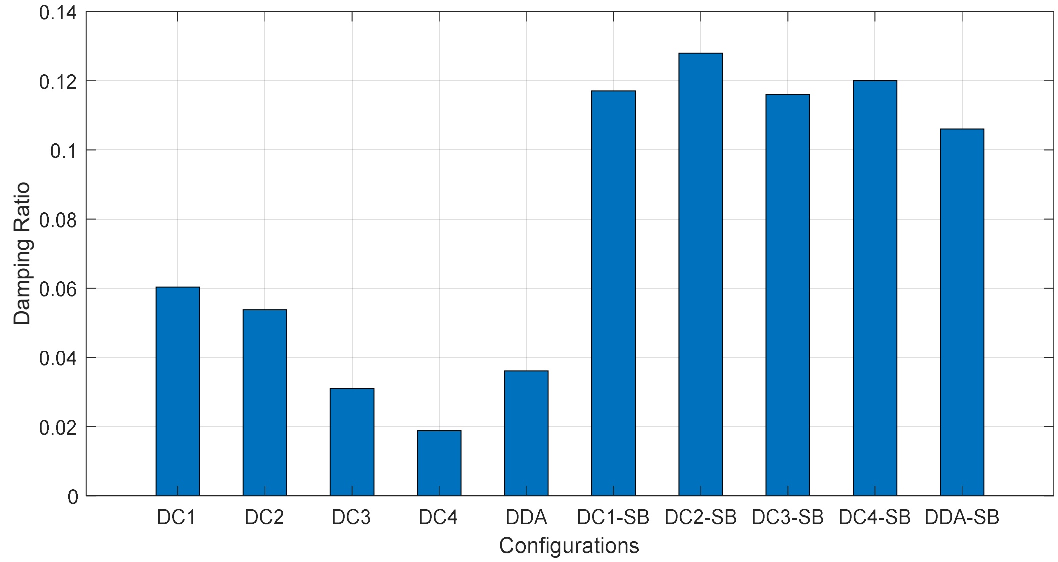

Figure 11: Estimated damping ratio of the structure with and without the strongback given the structural configurations used for the damper arrangement study

Figure 12 shows the maximum story drift calculated from the response of all the structure configurations in the damper arrangement study to the seven different ground motions considered. To compensate for the damping differences in the structure with and without the strongback, the maximum story drifts for all configurations and ground motions were normalized and plotted in Figure 13. For each ground motion, the maximum story drift was normalized by dividing by the maximum story drift from configuration DDA (for configurations without the strongback) or DDA-SB (for configurations with the strongback). The use of this normalization enables identification of the impact of the damper arrangement on the maximum story drift, controlling for differences in mass and damping.

The results in Figure 13 show that the largest and smallest normalized maximum drift without the strongback are 1.56 and 0.54 and the largest and smallest normalized maximum drift with the strongback are 1.22 and 0.88. The average normalized maximum story drift with concentrated dampers was found to be 1.06 for configurations without a strongback and about 1.00 for configurations with a strongback. Additionally, the standard deviation with concentrated dampers was found to be 0.26 for configurations without a strongback and 0.08 for configurations with a strongback. These results show that the placement and concentration of dampers has a large impact on the response of the system without the strongback; furthermore, with the dampers considered in this investigation, this included times where the impact is beneficial and other times where the impact is detrimental. In contrast these results also show that the placement and concentration of dampers has little effect on the system with a strongback.

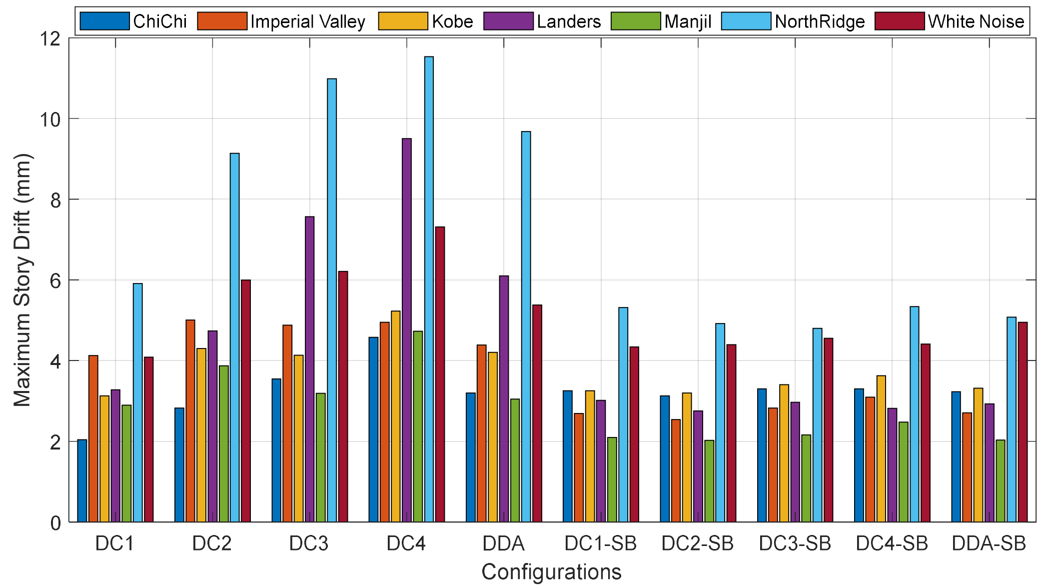

Figure 12: Maximum story drift from tests in the damper arrangement study.

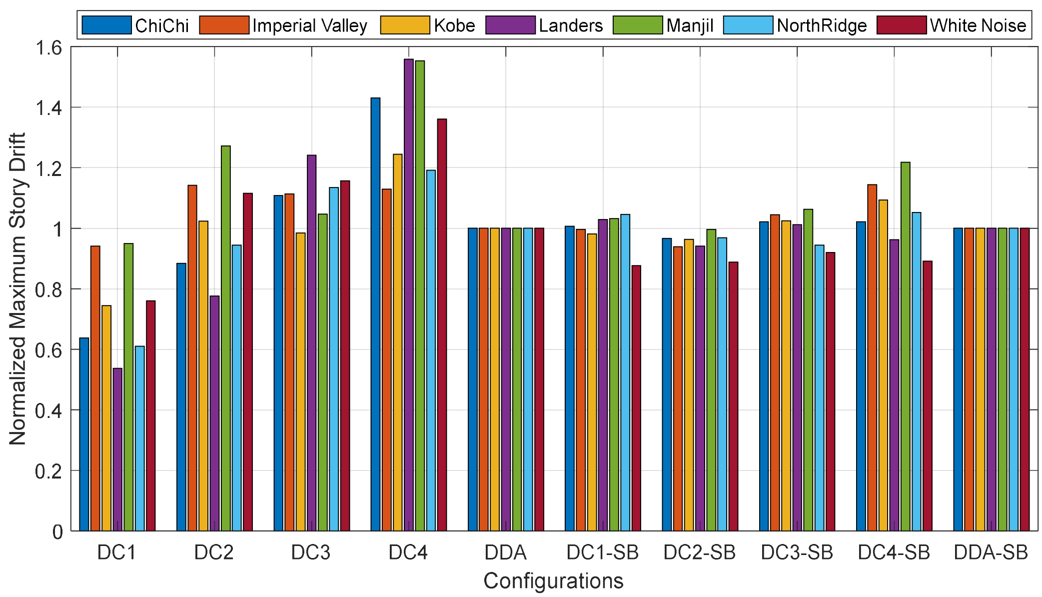

Figure 13: Normalized maximum story drift from tests in the damper arrangement study. Normalization of results from each record are performed with respect to the DDA configuration story drift results for systems without the strongback and with respect to the DDA-SB configuration story drift results for systems with the strongback

The normalized maximum roof drifts for all configurations and ground motions were calculated and are plotted in Figure 14. For each ground motion, the maximum roof drift was normalized with respect to the distributed dampers and no strongback configuration (DDA) for systems without a strongback and with respect to the distributed dampers with a strongback configuration (DDA-SB) for systems with a strongback. From the results in Figure 14, the average normalized maximum roof drift with concentrated dampers was found to be 1.04 for configurations without a strongback and 1.01 for configurations with a strongback. The standard deviation of the normalized maximum roof drift with concentrated dampers was found to be 0.26 for configurations without a strongback and 0.06 for configurations with a strongback. The consistency of the resulting normalized maximum story drift with the maximum roof drift both with the strongback and without the strongback indicates that this concentration of dampers does not lead to a large increase in concentration of localized story drift, which was seen considering stiffness irregularities.

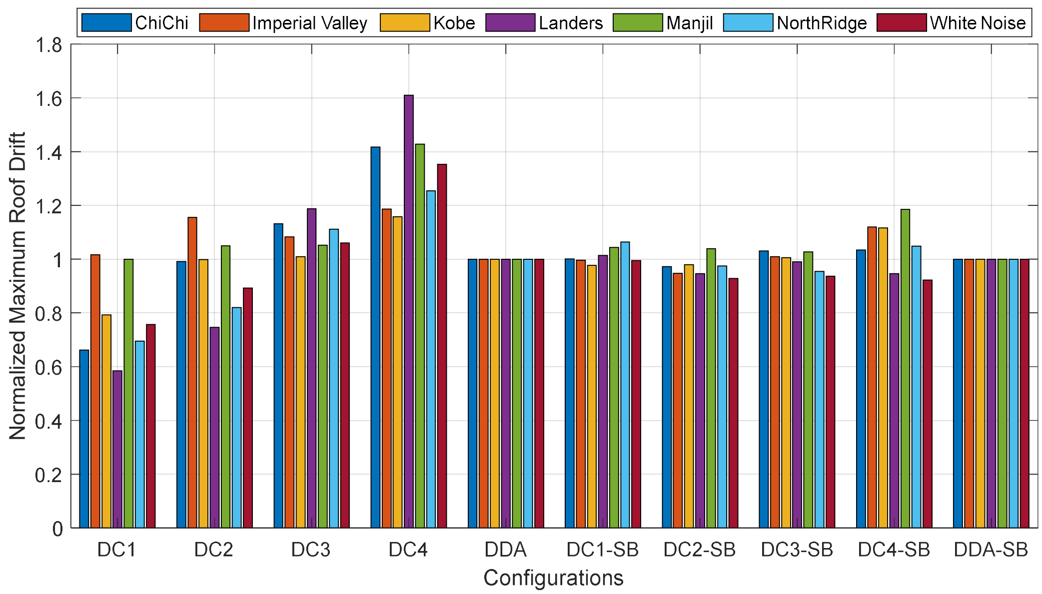

Figure 14: Normalized maximum roof drift from tests in the damper arrangement study. Normalization of results from each record are performed with respect to the DDA configuration roof drift results for systems without the strongback and with respect to the DDA-SB configuration roof drift results for systems with the strongback

Figure 15 shows the story drifts for all configurations in the damper arrangement study, with and without the strongback, and for all seismic records. This figure shows that, without the strongback, there are differences in the patterns and amplitudes of maximum story drift observed for the different damper arrangements, but, in general, story drifts are more concentrated in the lower stories of the structure. However, when a strongback is utilized, the drift is largely uniformly distributed across all stories for all seismic records and damper arrangements and the damper arrangement has a smaller impact on the amplitudes of the story drift.

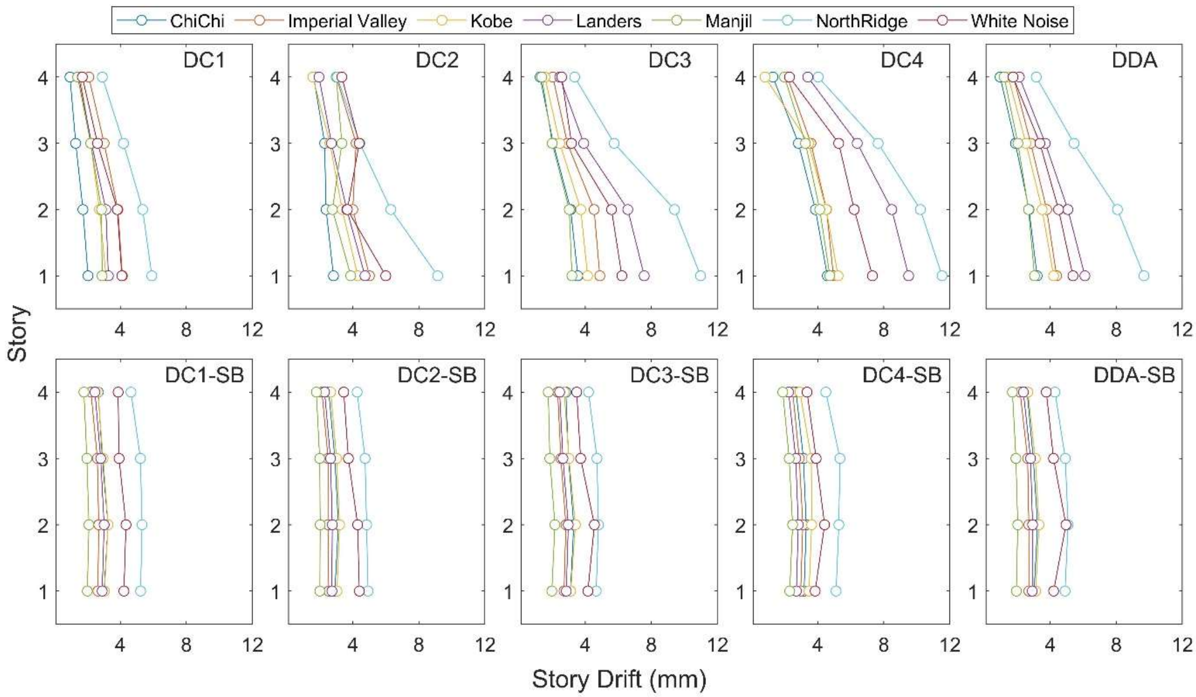

Figure 15: Story drifts of structure with and without strongback for all damper arrangement configurations and for all seismic records

5. Conclusions

The main focus of this work was to explore the impacts of damper arrangement and the location of soft story vertical stiffness irregularities on the dynamic behavior and properties of a structure with a strongback. The investigation was carried out through experiments conducted on a small-scale four-story structure that was subjected to ground motion generated by a shake table. This small-scale structure was tested with and without an attached strongback. The location of stiffness irregularities resulting from a reduction in column thickness at specific stories and the distribution of dampers at various stories of the structure were separately varied in the experiments. Maximum story and roof drift of the structure and the changes in its first natural frequency and damping were evaluated. As expected, due to the complex interaction of varying structural dynamics and ground motion dynamics, large variability in the results were observed considering the different ground motions. However, based on the results of this work, the following conclusions can be made:

- Without the strongback, the first mode frequency of the structure changed significantly depending on the location of the stiffness irregularity at different stories in the structure. In contrast, the inclusion of the strongback, a stiff elastic spine, resulted only in small changes in first mode frequency when evaluating the structure with stiffness irregularities at different stories.
- Without the strongback, the maximum story drifts were measured to be much higher on average than compared to with the strongback, even when controlling for the additional mass and damping of the strongback in the model.

- In both the stiffness irregularity study and the damper arrangement study, it was observed that the use of the strongback resulted in a largely uniform distribution of story drift along the height of the structure regardless of the stiffness irregularity or damper arrangement considered.
- The inclusion of the strongback resulted in consistency in the estimated first mode damping and maximum story drift when evaluating the structure with different damper arrangements.

The strongback's ability to protect against soft story vertical stiffness irregularities, regardless of their location, presents promising new options for structural design, architectural design, and the remediation of existing structures. Furthermore, the results of this work suggest that, with the strongback, energy dissipation devices can achieve similar levels of effectiveness if they are distributed throughout a structure or concentrated at one level or perhaps concentrated in a single large device. A topic of investigation that logically follows on the results of this study is the behavior of strongbacks combined with innovative energy dissipation devices that are well-suited to being concentrated. Also, the development of design methods for strongback systems that consider various distributions of energy dissipation devices and intentional stiffness irregularities is still needed.

Acknowledgments

The authors thank Paxton Lifsey for helping design the physical model used in this work and Griffin Barley for helping with the experimental testing.

This work was supported by the National Science Foundation under Grant No. 1940197. Any opinions, findings, and conclusions or recommendations expressed in this material are those of the authors and do not necessarily reflect the views of the National Science Foundation.

References

[1] M. S. Faramarzi and T. Taghikhany, "A comparative performance-based seismic assessment of strongback steel braced frames," *Journal of Building Engineering*, vol. 44, p. 102983, Dec. 2021, doi: 10.1016/j.jobe.2021.102983.

[2] B. G. Simpson and S. A. Mahin, "Experimental and Numerical Investigation of Strongback Braced Frame System to Mitigate Weak Story Behavior," *Journal of Structural Engineering*, vol. 144, no. 2, p. 04017211, Feb. 2018, doi: 10.1061/(ASCE)ST.1943-541X.0001960.

[3] B. Alavi and H. Krawinkler, "Strengthening of moment-resisting frame structures against near-fault ground motion effects," *Earthquake Engineering & Structural Dynamics*, vol. 33, no. 6, pp. 707–722, 2004, doi: 10.1002/eqe.370.

[4] G. S. Djojo, G. C. Clifton, and R. S. Henry, "Rocking steel shear walls with energy dissipation devices," presented at the 2014 NZSEE Annual Conference, 2014.

[5] M. R. Eatherton *et al.*, "Design Concepts for Controlled Rocking of Self-Centering Steel-Braced Frames," *Journal of Structural Engineering*, vol. 140, no. 11, p. 04014082, Nov. 2014, doi: 10.1061/(ASCE)ST.1943-541X.0001047.

[6] X. Chen, H. Tagawa, and J. A. S. Mateus, "Seismic performance of steel frame structure adopting parallel spine frames with elastic braces," *Engineering Structures*, vol. 267, p. 114640, Sep. 2022, doi: 10.1016/j.engstruct.2022.114640.

[7] S. Hu, W. Wang, and B. Qu, "Self-centering companion spines with friction spring dampers: Validation test and direct displacement-based design," *Engineering Structures*, vol. 238, p. 112191, Jul. 2021, doi: 10.1016/j.engstruct.2021.112191.

[8] T. Takeuchi, X. Chen, and R. Matsui, "Seismic performance of controlled spine frames with energy-dissipating members," *Journal of Constructional Steel Research*, vol. 114, pp. 51–65, Nov. 2015, doi: 10.1016/j.jcsr.2015.07.002.

[9] D. Slovenec, A. Sarebanha, M. Pollino, G. Mosqueda, and B. Qu, “Hybrid Testing of the Stiff Rocking Core Seismic Rehabilitation Technique,” *Journal of Structural Engineering*, vol. 143, no. 9, p. 04017083, Sep. 2017, doi: 10.1061/(ASCE)ST.1943-541X.0001814.
[10] M. Palermo, V. Laghi, G. Gasparini, S. Silvestri, and T. Trombetti, “Seismic Design and Performances of Frame Structures Connected to a Strongback System and Equipped with Different Configurations of Supplemental Viscous Dampers,” *Frontiers in Built Environment*, vol. 7, 2021, Accessed: Apr. 14, 2023. [Online]. Available: https://www.frontiersin.org/articles/10.3389/fbuil.2021.748087
[11] G. A. MacRae, Y. Kimura, and C. Roeder, “Effect of Column Stiffness on Braced Frame Seismic Behavior,” *Journal of Structural Engineering*, vol. 130, no. 3, pp. 381–391, Mar. 2004, doi: 10.1061/(ASCE)0733-9445(2004)130:3(381).
[12] B. G. Simpson and D. Rivera Torres, “Simplified Modal Pushover Analysis to Estimate First- and Higher-Mode Force Demands for Design of Strongback-Braced Frames,” *Journal of Structural Engineering*, vol. 147, no. 12, p. 04021196, Dec. 2021, doi: 10.1061/(ASCE)ST.1943-541X.0003163.
[13] A. Martin and G. G. Deierlein, “Generalized modified modal superposition procedure for seismic design of rocking and pivoting steel spine systems,” *Journal of Constructional Steel Research*, vol. 183, p. 106745, Aug. 2021, doi: 10.1016/j.jcsr.2021.106745.
[14] R. Montuori, E. Nastri, and V. Piluso, “Theory of plastic mechanism control: A new approach for the optimization of seismic resistant steel frames,” *Earthquake Engineering & Structural Dynamics*, vol. 51, no. 15, pp. 3598–3619, 2022, doi: 10.1002/eqe.3737.
[15] C. H. Chen, I. J. Tsai, and Y. Tang, “Drift Concentration of a Three-Story Special Concentrically Braced Frame with Strongback under Earthquake Loading,” *AMM*, vol. 863, pp. 287–292, Feb. 2017, doi: 10.4028/www.scientific.net/AMM.863.287.
[16] X. Chen, T. Takeuchi, and R. Matsui, “Seismic Performance and Evaluation of Controlled Spine Frames Applied in High-rise Buildings,” *Earthquake Spectra*, vol. 34, no. 3, pp. 1431–1458, Aug. 2018, doi: 10.1193/080817EQS157M.
[17] L. Fahnestock *et al.*, “U.S.-JAPAN COLLABORATION FOR SHAKE TABLE TESTING OF A FRAME-SPINE SYSTEM WITH FORCE-LIMITING CONNECTIONS,” in *17th World Conference on Earthquake Engineering, 17WCEE*, Sendai, Japan - September 27th to October 2nd, 2021, 2021. Accessed: Apr. 13, 2023. [Online]. Available: https://www.semanticscholar.org/paper/U.S.-JAPAN-COLLABORATION-FOR-SHAKE-TABLE-TESTING-OF-Fahnestock-Sause/8dc5985c7331d2c92c4ecc7cb6641081e080c76c
[18] J.-L. Lin, M.-K. Kek, and K.-C. Tsai, “Stiffness configuration of strongbacks to mitigate inter-story drift concentration in buildings,” *Engineering Structures*, vol. 199, p. 109615, Nov. 2019, doi: 10.1016/j.engstruct.2019.109615.
[19] S. S. Swain and S. K. Patro, “Seismic Protection of Soft Storey Buildings Using Energy Dissipation Device,” in *Advances in Structural Engineering*, V. Matsagar, Ed., New Delhi: Springer India, 2015, pp. 1311–1338. doi: 10.1007/978-81-322-2193-7_102.
[20] A. Siar Mahmood Shah and S. Moradi, “Cyclic response sensitivity of energy dissipating steel plate fuses,” *Structures*, vol. 23, pp. 799–811, Feb. 2020, doi: 10.1016/j.istruc.2019.12.026.
[21] L. Panian, N. Bucci, and B. Janhunen, “BRBM Frames: An Improved Approach to Seismic-Resistant Design Using Buckling-Restrained Braces,” pp. 632–643, Dec. 2015, doi: 10.1061/9780784479728.052.
[22] N. Mashhadiali, S. Saadati, S. A. M. Mohajerani, and P. Ebadi, “Hybrid braced frame with buckling-restrained and strong braces to mitigate soft story,” *Journal of Constructional Steel Research*, vol. 181, p. 106610, Jun. 2021, doi: 10.1016/j.jcsr.2021.106610.
[23] Z. Qu, A. Wada, S. Motoyui, H. Sakata, and S. Kishiki, “Pin-supported walls for enhancing the seismic performance of building structures,” *Earthquake Engineering & Structural Dynamics*, vol. 41, no. 14, pp. 2075–2091, 2012, doi: 10.1002/eqe.2175.

[24] X. Wang, Z. Qu, and T. Gong, “Role of dampers on the seismic performance of pin-supported wall-frame structures,” *Earthq. Eng. Eng. Vib.*, vol. 22, no. 2, pp. 453–467, Apr. 2023, doi: 10.1007/s11803-022-2092-5.

[25] Lifsey, P., Drake, C., Wierschem, N., Abolghasemi, S., and Denavit, M., “Structural Design Drawings.” in Impact of strongback on structure with varying damper and stiffness irregularity arrangements, DesignSafe-CI, 2023. doi: 10.17603/ds2-r5wm-6b46.

[26] T. D. Ancheta *et al.*, “NGA-West2 Database,” *Earthquake Spectra*, vol. 30, no. 3, pp. 989–1005, Aug. 2014, doi: 10.1193/070913EQS197M.

[27] F. Alemdar and F. M. A. Al-Gaadi, “Experimental Study of Earthquake Simulator for 3D Cold-Formed Steel Frame Structure,” *Lat. Am. j. solids struct.*, vol. 19, p. e426, Jan. 2022, doi: 10.1590/1679-78256812.

[28] A. B. K. Teh and C. Venkatratnam, “Design and development of a seismic shaking table for evaluation and analysis of the performance of elastomeric bearing,” in *2015 IEEE Student Conference on Research and Development (SCOReD)*, Dec. 2015, pp. 111–116. doi: 10.1109/SCORED.2015.7449306.

[29] A. Maree *et al.*, “Shaking Table Experiments of Dry Storage Casks,” Aug. 2015.

[30] X. Lu, Y. Chen, and Y. Mao, “Shaking table model test and numerical analysis of a supertall building with high-level transfer storey,” 2012, doi: 10.1002/tal.632.

[31] D. Lignos, “Sidesway collapse of deteriorating structural systems under seismic excitations,” Ph.D., Stanford University, United States -- California, 2008. Accessed: Jul. 13, 2022. [Online]. Available: https://www.proquest.com/docview/304469377/abstract/201B72AF97E74781PQ/1

[32] X. Lu, Y. Zhou, and F. Yan, “Shaking Table Test and Numerical Analysis of RC Frames with Viscous Wall Dampers,” *Journal of Structural Engineering*, vol. 134, no. 1, pp. 64–76, Jan. 2008, doi: 10.1061/(ASCE)0733-9445(2008)134:1(64).

[33] C. S. Li, S. S. Lam, M. Z. Zhang, and Y. L. Wong, “Shaking Table Test of a 1:20 Scale High-Rise Building with a Transfer Plate System,” *Journal of Structural Engineering*, vol. 132, no. 11, pp. 1732–1744, Nov. 2006, doi: 10.1061/(ASCE)0733-9445(2006)132:11(1732).

[34] The MathWorks Inc, “MATLAB version: 9.9 (R2020b).” The MathWorks Inc., Natick, Massachusetts, United States, 2020. [Online]. Available: https://www.mathworks.com

[35] The MathWorks Inc, “System Identification Toolbox version: 9.13 (R2020b).” The MathWorks Inc., Natick, Massachusetts, United States, 2020. [Online]. Available: https://www.mathworks.com